Chapter-3

To study the drying behavior of fresh haritaki (Terminalia chebula) fruit

3.1. Introduction

In South East Asia, particularly India, *Terminalia chebula Retizus* (*Combretaceae*) is commonly cultivated. Its common name is “chebulic myrobalan”. In Sanskrit it is known as "Haritaki" while as in Hindi it is referred as “Harad”. Due to its exceptional healing abilities, it has been referred to as the “King of Medicine” since ancient times and occupies the highest position in the list of “Ayurvedic Materia Medica” [61]. However, origin of this fruit is the northern light rainfall forests of India, in present day Uttar Pradesh and West Bengal and is common crop in Tamil Nadu, Karnataka and Southern Maharashtra. It has been utilized as a remedy to treat illnesses ever since the dawn of time. April-August and September-January are the flowering and fruiting seasons, respectively. The flowering season is from April to August, while the fruiting season is from September to January. Its drupe-like fruit measures length 2-4.5 cm and breadth 1.2-2.5 cm, respectively, with tinge of black or yellowish-brown spot and have five longitudinal ridges. The fruit has an astringent, acidic, and sweet flavour and is starchy and fibrous [64]. Therapeutic activities of *T. chebula* have included hypocholesterolaemia, anti-inflammatory, anti-allergic, antibacterial, and antioxidant effects, among others [33, 66]. These characteristics result from the fruit’s content of phytochemicals, particularly phenolics and flavonoids [66]. Owing to the antioxidative attributes of *T. chebula* a number of researchers have indicated interest in employing it as a phytotherapy. Additionally, as it is a seasonal fruit, fruit drying is important and serves as an alternate preservation technique that lengthens the fruit's shelf life [51].

Drying is an important preservation technique in which mass and heat exchange/transfer happens between drying air and inside of the material at the same time. It is accompanied with variation in material and prevent potential degradation, contamination, and other factors during extended storage periods [48]. The drying phenomenon represented by thin layer drying models of agricultural products is identified as theoretical and empirical [55]. Simple techniques like sun drying or mechanical dryers like tray dryers could be used to dry agricultural produce [4]. Different biological materials have different physiochemical properties, which necessitates adjusting the drying processes and parameters to match the requirements for the final product’s quality [49]. Sun drying has some drawbacks, including a greater labour cost, a need for a broad area, contamination and bug infestations which could inflict sickness or damage, and a lengthier drying time, especially during wet seasons [40]. Many industrial drying

procedures employ tray drying because it is faster and more uniform than solar drying [47]. The information on moisture diffusivity is used to plan the mass transfer in the drying process, calculate activation energy, and assess the relative ease with which moisture migrates within the product. Few studies have been done up to this point on drying and the creation of value-added products from *T. chebula* fruit [19]. Water activity is a factor during degradation reactions. This water activity depends on the biosystems of both on water content and the properties of the diffusion surface [5]. While drying aids in the preservation of plant materials, it negatively affects several of their key chemical components, such as phenolic compounds, vitamins, and colours [73]. The final grade of the plant material is determined by the percentage of original colour and other chemicals retention after drying. Therefore, in order to produce dried products with improved qualities like antioxidant activity, it becomes vital to analyse the kinetics of these components degradation and colour change during drying. There is currently no literature on *T. chebula* drying, despite the fact that drying and degradation kinetics for a variety of agricultural and industrial items under various drying settings have been described [53, 73]. Williams [79] found that the majority of underutilised fruits and vegetables are versatile foods. Indian ayurvedic medicine uses triphala, a herbal mixture made from the fruits of 3 different trees (*Embilica officinalis, Terminalia chebula,* and *Terminalia bellerica*), to treat various diseases due to its enormous biological properties [52].

Unfortunately, there aren't many value-added items on the market right now. Therefore, for these kinds of foods, effective packaging and storage system design is crucial. Moisture sorption isotherm (MSI) studies are thought to be one of the most effective methods for figuring out the best conditions for storage and packing in order to maximise biological stability and product quality retention [20]. The food's MSI is determined by the connection between its moisture content and water activity at a constant temperature. When the material achieves equilibrium through wetting or drying, respectively, adsorption and desorption isotherms are referred to [77]. A dry substance is maintained in an environment with rising (RH) relative humidity, and gaining the weight brought on by moisture absorption is measured to determine the adsorption isotherm. The desorption isotherm, on the other hand, is calculated by maintaining an initially wet material at the same relative humidity conditions and measuring the weight loss [6]. To predict food MSI different mathematical models including both semi-empirical and empirical ones have been proposed [16, 58, 72].

In order to control deteriorative processes viz. microbial contamination and spoilage, lipid oxidation, etc. during storage for long term, this chapter emphasises the engineering properties and evaluates the drying kinetics of *T. chebula* fruits at different temperatures as well as assesses the degradation kinetic of phytochemicals, colour, etc. by fitting them in various mathematical models and moisture sorption isotherm. These mathematical models would be helpful in forecasting how phytochemicals will behave during drying and in studying how *T. chebula* fruit can be used for diverse industrial applications.

3.2. Materials and methods

3.2.1. Materials

The matured haritaki fruit was collected from the horticulture section, Tezpur University, Assam, India. All of the analytical grade reagents used for analysis were purchased from Merck-Sigma, India. In order to remove any dirt that had adhered to the fruits, they were washed with distilled water.

3.2.2. Engineering properties of the fruit

The freshly harvested fruits were characterized for mass using an analytical balance (TB 215DDE, Denver), geometrical properties including average length (L), breadth (B), and thickness (T) using digital electronic carbon fiber Venire caliper (Generic, LSHAZI03590) and weight (Wt). Equation was used to calculate engineering properties like arithmetic mean diameter (AMD, D_A), geometric mean diameter (GMD, D_G), sphericity (ψ), aspect ratio, surface area (SA) and volume [15, 37]. The average length and thickness were used to determine H. Equation were used for the calculation of minimum and maximum radius of curvature [15].

$$D_A = \left(\frac{L + B + T}{3}\right) \tag{3.1}$$

$$D_G = LBT^{1/3} \tag{3.2}$$

$$S(\psi) = \frac{D_G}{L} \times 100 \tag{3.3}$$

$$Aspect\ ratio = \frac{B}{L} \times 100 \tag{3.4}$$

$$SA = \pi D_{G^2} \tag{3.5}$$

$$V = \frac{\pi}{6} D_{G^3} \tag{3.6}$$

$$H = \frac{T + L}{2} \tag{3.7}$$

$$R_{min} = \frac{H}{2} \tag{3.8}$$

$$R_{max} = \frac{H^2 + \frac{L^2}{4}}{2} \tag{3.9}$$

3.2.3. Drying of sample

Drying behaviour of *T. chebula* fruit was studied by using a laboratory tray dryer (Labotech, BDI-51, B. D. Instrumentation, Ambala, India) at five different temperatures (40, 50, 60, 70 and 80 °C). The seeds from the fresh *T. chebula* fruits were first removed using a knife by cutting it into half and were sliced into 2 mm slices. The sliced fruit were placed in the tray of the drying chamber in single layer and kept for drying. The change in the weight of the sample during drying process was estimated at an interval of 15 min till it attains equilibrium moisture content (EMC). All the experiments were carried out in triplicates.

3.2.4. Moisture content

The samples were maintained in a hot air oven for 24 h at 105 °C to achieve constant weight in order to determine the moisture content [60]. The samples original moisture content was discovered to be 75.56±1.16% (wet basis).

3.2.5. Mathematical modelling

Effective modelling of the drying process is required to ascertain the drying behaviour of *T. chebula* fruit. The models that best match the drying curves of the samples are those that do so. The best fit model and the goodness of fit are determined using statistical parameters such the reduced root mean square error (RMSE) value and coefficient of determination (R^2) values [29]. Typically, the best model is the one with the lowest RMSE and highest R^2 value [34]. In the present study seven different thin layer drying models as listed in (**Table 3.1.**) were chosen for fitting the experimental drying data of haritaki fruit in tray dryer at different temperatures. Moisture ratio is calculated by following equation:

$$MR = \frac{M_t - M_e}{M_0 - M_e} \tag{3.10}$$

where, MR = Moisture ratio, M_t = Moisture content of sample at any time (kg water/ kg dry matter), M_o = Initial moisture content (kg water/kg dry matter), M_e = Equilibrium moisture

content (kg water/kg dry matter), According to literature, the value of (M_e) equilibrium moisture content are relatively small as compare to (M_t) moisture content of sample and (M_o) initial moisture content for long drying, so MR moisture ratio can be simplified to M_t/M_o [45].

$$MR = \frac{M_t}{M_0} \tag{3.11}$$

Table 3.1. Mathematical models fitted to the thin layer drying curve of *T. chebula* fruit

Sl. No.	Models Name	Model equation (MR)	References
1.	Newton	$e^{(-kt)}$	Westerman et al. [78]
2.	Page	$e^{(-kt^n)}$	Page [54]
3.	Logarithmic	$a * e^{(-kt)} + c$	Yaldiz et al. [83]
4.	Approximation of diffusion	$a * e^{(-kt)} + (1-a) * e^{(-kbt)}$	Yaldiz et al. [83]
5.	Verma et al	$a * e^{(-kt)} + (1-a) * e^{(-gt)}$	Verma et al. [76]
6.	Midilli et al	$a * e^{(-kt^n)} + bt$	Midilli et al. [46]
7.	Diffusion	$a * e^{(-bt)}$	Tulek [70]

3.2.6. Moisture diffusivity

Fick's second law of diffusion, which is widely acknowledged for characterising the period of time when the rate of drying falls, is used extensively to examine the thin layer drying of food ingredients [70]. Based on the Fick's 2nd law of diffusion, drying curves for moisture ration versus drying time for thin layer drying at different drying air temperatures and the effective moisture diffusivity was calculated from the curves.

$$MR = \frac{8}{\pi^2}\sum_{n=0}^{\infty} \frac{1}{(2n+1)^2}\ exp - \left(\frac{(2n+1)^2\pi^2 D_{eff} t}{4L^2}\right) \tag{3.12}$$

where, D_{eff} the effective diffusivity (m^2/s), L is thickness of layer (m). Equation **(3.12)** can be simplified by taking the first term of Eq. **(3.13)**:

$$MR = \frac{8}{\pi^2} exp\left(-\frac{\pi^2 D_{eff} t}{4L^2}\right) \tag{3.13}$$

A useful measure of moisture diffusion Plotting ln (MR) with drying time from the experimental data allowed us to get the D_{eff} value. The figure shows a straight line with a downward slope, and "K" is connected to "D_{eff}" by Eq. **(3.14)**

$$K = \frac{\pi^2 D_{eff} t}{4L^2} \tag{3.14}$$

3.2.7. Activation energy

The energy used to eradicate one mole of moisture from a substance with a certain moisture content and a similar composition is known as activation energy [26]. An Arrhenius type equation was employed to predict the dependence of the effective moisture diffusivity (D_{eff}) on the drying temperature as follows:

$$D_{eff} = D_0 exp\left(-\frac{E_a}{\mathrm{RT}}\right) \tag{3.15}$$

where, D_0 = effective moisture diffusivity at infinite temperature (m^2/s), E_a = activation energy for diffusion (kJ/mol), R = gas constant (8.314×10^{-3} kJ/ mol), T = temperature (K).

3.2.8. Phytochemical determination

3.2.8.1. Extract preparation

Methanolic extracts of the samples were produced to assess the antioxidant and phytochemical activities. Water and solvent were diluted 50:50 (v:v) to make the solvent concentration. The extract was then filtered through Whatman no. 1 filter paper. Later, the extract was concentrated using a rotary evaporator at 40 °C (rpm 200) under decreased pressure (Equitron, Roteva, Medica Instrument Mfg. Co., Mumbai, India). To provide protection from heat and light the extracts were kept at - 4 ℃ in a dark bottle.

3.2.8.2. Total phenolic content (TPC)

TPC was calculated using the procedure outlined by Kim et al. [38]. In a nutshell, 9 mL of deionized water were combined with 1 mL of the extract. The extract received 1 mL of Folin-phenol Ciocalteu's reagent, which was then shaken. After 5 min, 10 millilitres of a 7% Na_2CO_3 solution were added. The mixture was completely mixed and promptly diluted with deionized water to a volume of 25 mL. 90 min at 40 °C were spent incubating the combined solution. After incubation, at 750 nm the absorbance was

measured. Gallic acid was used as a standard for the calculation of total phenolic (0–100 mg/L) and expressed as mg of gallic acid equivalents (GAE) per g of dried sample.

3.2.8.3. Total flavonoid content (TFC)

The modified Dewanto et al. [21] technique was used to determine the total flavonoid content. 3 mL of the extract and 0.3 mL of the 5% $NaNO_2$ solution were combined. After five minutes, 0.6 mL of 10% $AlCl_3$ solution and 2 mL of NaOH solution were added (1 M). After the solution had been vortexed, the absorbance at 510 nm was determined. TFC was expressed as mg of Quercetin equivalent (mg of QE) per g of dry matter taken.

3.2.8.4. Total antioxidant activity (DPPH radical scavenging activity)

The method of Brand-Williams et al. [12] was modified to calculate the total antioxidant activity using the DPPH assay. 100 µL of the extract were combined with 3 mL of DPPH solution. The test tube's solution was well agitated and heated to 40 °C in the dark for 20 min. Then, at 517 nm the absorbance was measured and total antioxidant activity was determined by using the following equation:

$$\text{Total antioxidant activity (\%)} = \frac{\text{Absorbance of standard} - \text{Absorbance of sample}}{\text{Absorbance of standard}} \times 100 \quad (3.16)$$

3.2.8.5. Vitamin C

By using the titration method outlined by Ranganna [60], the vitamin C content was calculated and reported as mg vitamin C/100 g dry matter.

3.2.9. Colour measurement

Using Hunter Colour Lab, the colour of the fruit slices was assessed periodically as they dried (Hunter Associates Laboratory Inc., Reston, VA, USA). L* (lightness to darkness), a* (redness to greenness), and b* were used to express the colour values (yellowness to blueness). Total colour difference (ΔE^*) were calculated using following equation:

$$\Delta E^* = [(\Delta E^*)^2 + (\Delta E^*)^2 + (\Delta E^*)^2]^{1/2} \quad (3.17)$$

3.2.10. Degradation kinetics

Experiments for the degradation investigation were conducted at three distinct temperatures, namely 60, 70 and 80 °C. The following first-order kinetic model was used

to match the experimental data for TPC, TFC, DPPH radical scavenging activity, and colour change as described below:

$$C = D_0 e^{\pm kt} \quad (3.18)$$

where C_0 is the parameter values before the drying process began and C represents the TPC, TFC, DPPH radical scavenging activity, and colour difference throughout drying. First order kinetic rate constant is denoted by "k" Following are the results of the calculations made for the half-life ($t_{1/2}$) of phytochemical degradation and colour change

$$t_{1/2} = ln2/k \quad (3.19)$$

The Arrhenius equation was used to assess how temperature affected antioxidant properties, colour change, and phytochemical degradation.

$$k = k_0 e^{E_a/RT} \quad (3.20)$$

Where, E_a is the activation energy (kJ/mol), R is ideal gas constant (8.3145×10^{-3} kJ/mol. K), T is temperature (K).

3.2.11. Determination of sorption isotherm

The equilibrium moisture content of haritaki pulp powder was measured using the static gravimetric method at eight relative humidity levels between 7 and 85% that were maintained by saturated salt solutions of NaOH, LiCl, $MgCl_2$, $K(CO_3)_2$, $Mg(NO_3)_2$, KI, NaCl, and KCl [27]. Beakers with weight inside were inserted into airtight glass jars with saturated salt solutions, ensuring level of solution below beaker necks. Samples (2 g each) were retained in a small container and added to the beakers after the beakers had been properly immersed in the solutions. The jars were then sealed with lids and kept at different temperatures (30, 40 and 50 ^oC). When the weight change between two readings was less than 0.001 g, the equilibrium condition was determined. Data analysis employed measurements from three duplicate samples. A petri dish was kept in a separate jar with RH >75%, for evaluate the possible mould growth [42].

3.2.12. Modelling of sorption isotherms

To create sorption isotherms, the equilibrium moisture content of haritaki pulp powder and the related water activity were shown at three different temperatures. For fitting sorption data, eight different sorption models that have been utilised successfully in several studies involving foods that are comparable to one another were selected (**Table 3.2**) [27, 39, 50, 68, 74].

Table 3.2. Moisture sorption isotherm models used to fit experimental EMC-ERH data for haritaki pulp powder

Sl. No.	Models Name	Mathematical expression	References
1.	GAB (Guggenheim-Anderson-de Boer)	$M_e = \frac{M_0 C K a_w}{(1 - K a_w)(1 - K a_w + C K a_w)}$	Van Den Berg and Bruin [72]
2.	BET (Brunauer-Emmett-Teller)	$M_e = \frac{M_0 C a_w}{(1 - a_w)[1 + (C - 1)a_w]}$	Brunauer et al. [14]
3.	Modified Henderson	$M_e = \{\ln(1 - a_w) / [-A(T + B)]\}^{1/C}$	Thompson [69]
4.	Peleg	$M_e = k_1 a_w^{n_1} + k_2 a_w^{n_2}$	Peleg [57]
5.	Iglesias & Chirife	$M_e = A + B \frac{a_w}{1 - a_w}$	Chirife and Iglesias [17]
6.	Modified Oswin	$M_e = (A + BT)\left(\frac{a_w}{1 - a_w}\right)^C$	Andrade et al. [8]
7.	Caurie Model	$M_e = e^{(A + B * a_w)}$	Caurie [16]
8.	Smith Model	$M_e = A - B * (\ln(1 - a_w))$	Martínez-Las Heras et al. [44]

A non-linear least-squares regression analysis was utilised to evaluate the models. The curve fitting and regression analysis were done using the programme Origin-Pro 9.1. To evaluate the accuracy of fit for models, the sum of square errors attributable to fit (SSE), percent root mean square error (RMSE), reduced chi-square (χ^2), and adjusted correlation coefficient (R^2) values were utilised. The best match was determined to be the equation with the lowest R^2, SSE, RMSE, and modified R^2 values. The calculation of the error metrics in terms of SSE, RMSE, χ^2, and R^2 **(Eq. 3.21-3.25)**, [68].

$$SSE = \sum_{i=1}^{n} w_i \left(M_i - \widehat{M}_i\right)^2 \quad (3.21)$$

$$SST = \sum_{i=1}^{n} w_i (M_i - \bar{M}_i)^2 \quad (3.22)$$

$$RMSE = \sqrt{\frac{SSE}{n-m}} \quad (3.23)$$

$$\chi^2 = \sum_{i=1}^{n} \frac{(M_i - \overline{M_i})^2}{\sigma_i^2} \quad (3.24)$$

$$R_{adj}^2 = 1 - \frac{SSE(n-1)}{SST(n-m)} \quad (3.25)$$

Where, w_i is the weight assigned to each data point in this analysis, which was set to unity, and M_i is the experimental EMC, $\widehat{M}_i$ is the predicted EMC from the fitting curve, SST stands for "Total Sum of Square Value" "n" denotes "experimental Data Point" and "m" denotes "M" coefficients in each equation.

In accordance with water activity, the standardised residuals (difference between measured and projected moisture content) were calculated **(Eq. 3.21)**. The residual plots revealed whether there was a clear pattern or randomly. When the residual points are centered on the origin in the horizontal plane, a model is regarded as valid.

3.2.13. Statistical analysis

The mean and standard deviation are used to present all the data.

3.3. Results and discussion

3.3.1. Engineering properties of the haritaki fruit

The engineering properties of haritaki with the maximum, minimum, mean along with SD values are tabulated in **Table 3.3**. According to the current study, haritaki fruits were 4.10±0.25, 1.83±0.08, and 1.58±0.10 cm in length, breadth, and thickness, respectively. The typical AMD and GMD for haritaki were measured to be 2.50±0.09 cm and 3.95±0.39 cm, respectively. These average diameters can be used to calculate the size of the machine's aperture for fruit segregation as well as the fruit particle moving for projected area through a turbulent zone of an air stream. The surface of the haritaki was measured as having a mean value of 49.47±9.64 cm^2, with the smallest area being 34.50 cm^2 and the biggest being 61.23 cm^2. The free flow ability, appropriate handling, and grading design of food commodities are typically determined by their sphericity, which is also frequently used to indicate the shape of the item [15, 37]. The fruit was shaped using measurements of sphericity and aspect ratio. It was discovered that haritaki's aspect ratio was 44.77±3.18%. The equipment for size and separation must be designed with consideration for sphericity. The aspect ratio and sphericity of the fruit can be used to analyse its flow ability properties. Therefore, these two factors affect how fruit flows [59]. Fruit is deemed to be spherical in shape at or more than 0.80 sphericity value [10]. Haritaki fruit will slide on the designated surface rather than scroll down, as evidenced by its low sphericity score of 0.84. The propensity of the fruit to roll or slide is a crucial element in the construction of hoppers [56]. Burubai and Amber [15] suggested that food products with a high aspect ratio and low sphericity slide more readily than they roll on

flat surfaces. Aspect ratio and sphericity values are useful for designing chutes and hoppers. In the design of machinery like sorters, which are based on the height of food items, the radius of curvature is regarded as one of the crucial design factors. The volume of the haritaki was determined to be 33.13±9.44 cm^3. Calculations revealed that the R_{min} was 49.47±9.64 cm^2 and the R_{max} was 1.42±0.06 cm.

Table 3.3. Engineering properties of haritaki fruit

Sl. No.	Properties	Unit	No. of observations	Minimum	Maximum	Mean	Standard deviations
1.	Length (L)	(cm)	10	3.80	4.50	4.10	0.25
2.	Breadth (B)	(cm)	10	1.70	2.00	1.83	0.08
3.	Thickness (T)	(cm)	10	1.40	1.70	1.58	0.10
4.	Weight (Wt)	(g)	10	6.62	10.05	7.90	1.25
5.	Sphericity S (ψ)	(%)	10	84.00	107.66	96.43	8.32
6.	Aspect Ratio (AR)	(%)	10	39.13	48.78	44.77	3.18
7.	Surface area (SA)	(cm^2)	10	34.50	61.23	49.47	9.64
8.	Minimum radius (R_{min})	(cm)	10	1.35	1.50	1.42	0.06
9.	Maximum radius (R_{max})	(cm)	10	9.09	12.25	10.18	1.01
10.	Geometric mean diameter (GMD, D_G)	(cm)	10	3.31	4.41	3.95	0.39
11.	Arithmetic mean diameter (AMD, D_A)	(cm)	10	2.36	2.66	2.50	0.09
12.	Volume (V)	(cm^3)	10	19.05	45.03	33.13	9.44

To design conveying, separating, grading, packing, cutting, etc. equipments physical features of the fruit viz. as size, density, colour, surface area, appearance, porosity, shape etc. are taken into consideration [65, 67]. Fruit's mechanical and textural properties help with equipment design, fruit sorting, and fruit quality assessment for consumption [62]. In order to minimise post-harvest losses, knowledge on engineering features, such as mechanical, textural, physical, thermal, frictional, properties, is most helpful in the processing of agricultural products. This is true for developing equipment for post-harvest processing, processing of value-added goods, processing of fruits industrially, and for simple handling, transportation, packing, and storage [63, 62].

3.3.2. Fitting of drying curves

Fig. 3.1. depicts the variations in moisture ratio with drying time for drying of *T. chebula* fruit at 40, 50, 60, 70 and 80 °C. According to the findings, drying time dropped as drying air temperature rose because heat transfer rates increased along with it, speeding up the movement of water molecules out of the pulp. When the air temperature was raised from 40 to 80 °C, the drying time for fruit samples dropped from 750 to 285 min. The outcomes concur with those for Cape gooseberry and Cornelian cherry [75, 82]. The drying time was plotted along with the drying curve and the dimensionless moisture ratio. As drying time lengthens, then immediate moisture content rapidly falls down ward. With longer drying times, a drop in drying rate was seen. The moisture ratio was also shown to be steadily declining. Early on in the drying process, when the moisture content was highest, it was discovered that the drying rate was very high. However, when the moisture ratio reduced, the drying rate began to decline.

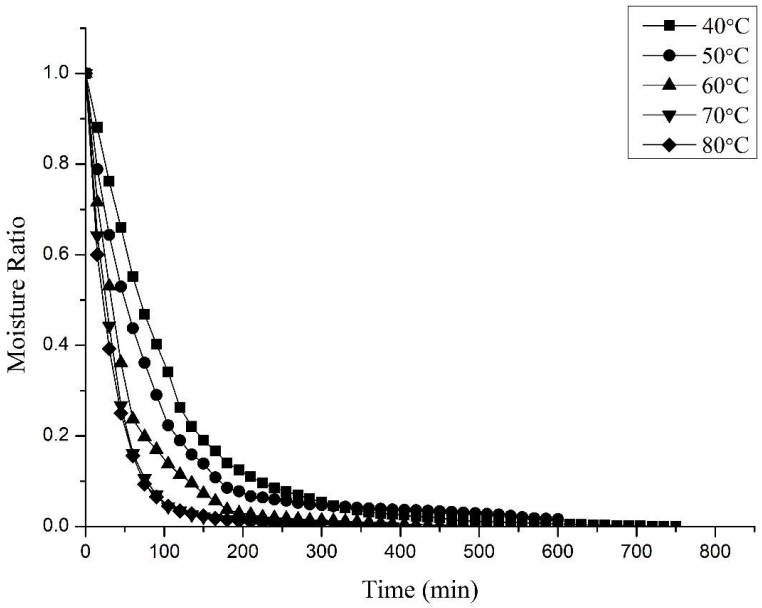

Fig. 3.1. Variation in moisture ratio vs time for *T. chebula* fruit at different temperatures

However, when the surface began to dry, the water that was already there started to be withdrawn, making it impossible for the surface to remain saturated. This is because the pace at which water is moving to the surface is insufficient to keep it saturated. As a result, the drying rate was reduced since the surface was not in an equilibrium state [13]. Following the rapid decline phase of the drying rate, the drying rate again decreases until it achieves the equilibrium moisture content when the moisture level falls below the critical moisture content during the falling rate period. Numerous studies on aromatic plants produced similar findings [3, 11]. The drying process, as shown by these graphs, did not have a constant rate phase; rather, nearly the whole drying process occurred during a falling rate phase, starting from the initial moisture content (74.82% dry basis) to the end moisture content (3.96% dry basis). Similar outcomes were found in past investigations on various fruits [2, 24].

3.3.3. Drying model evaluation

Seven distinct drying models were subjected to non-linear regression analysis, and the statistical findings for the models and the model coefficients are reported in **Table 3.4**. Highest average R^2 and lowest average RMSE for a model for the various temperatures were the criteria for choosing the best model. While RMSE ranged from 0.0084 to 0.0141, the average R^2 ranged from 0.9955 to 0.9986. The 'Approximation of Diffusion' model was discovered to best fit the experimental data based on the selected criteria.

Table 3.4. Model and statistical parameters obtained from fitting of drying models for convective drying of *T. chebula* fruits

Model	Temperatures (°C)	Model parameters			R^2	Average R^2	RMSE	Average RMSE
Newton	40	k = 0.0103			0.9977	0.9955	0.01147	0.01409
	50	k = 0.01351			0.9891		0.02350	
	60	k = 0.02089			0.9937		0.01758	
	70	k = 0.02893			0.9988		0.00799	
	80	k = 0.03125			0.9985		0.00991	
Page	40					0.9971		0.01161
	50	k= 0.008435	n = 1.042		0.998		0.01069	
	60	k = 0.02407	n = 0.8713		0.9928		0.01933	
	70	k = 0.03413	n = 0.8795		0.9965		0.01323	
	80	k = 0.028	n = 1.009		0.9988		0.00811	
		k = 0.04133	n = 0.9246		0.9994		0.00667	
Logarithmic	40					0.9983		0.00908
	50	k = 0.01077	a = 1.022	c = 0.005858	0.9984		0.00971	
	60	k= 0.01471	a = 0.9635	c = 0.02927	0.999		0.00724	
	70	k = 0.02146	a = 0.9762	c = 0.0121	0.9959		0.01458	
	80	k = 0.02943	a = 0.9982	c = 0.004844	0.9991		0.00719	
		k = 0.03193	a = 0.9835	c = 0.009213	0.9994		0.00669	
Approximation of diffusion	40					0.9986		0.01125
	50	k = 0.01045	a = 0.995	b = 0.02401	0.9979		0.00677	
	60	k = 0.01527	a = 0.9531	b = 0.07069	0.9991		0.01004	
	70	k = 0.02787	a = 0.7649	b = 0.3481	0.998		0.00833	
	80	k = 0.03389	a = 0.1922	b = 0.8228	0.9988		0.00560	
		k = 0.03425	a = 0.9376	b = 0.2796	0.9996		0.00840	

Midilli et al	40	k = 0.008591	a = 1.013	b = 0.0000119	n = 1.043	0.9985	0.9985	0.00941	0.00897
	50	k = 0.01789	a = 1	b = 0.0000558	n = 0.945	0.9984		0.00941	
	60	k = 0.03383	a = 1.009	b = 0.000014	n = 0.8851	0.9969		0.01290	
		k = 0.02698	a = 0.999	b = 0.0000168	n = 1.019	0.9991		0.00746	
	70	k = 0.03928	a = 0.9993	b = 0.0000256	n = 0.94	0.9996		0.00564	
	80								
Diffusion	40	a = 1.023	b = 0.01054			0.9981	0.9958	0.01052	0.01377
	50	a = 0.971	b = 0.01309			0.9898		0.02300	
	60	a = 0.9803	b = 0.02046			0.994		0.01739	
		a = 1.001	b = 0.02896			0.9988		0.00814	
	70	a = 0.9889	b = 0.03091			0.9986		0.00977	
	80								
Verma et al	40	k = 0.01054	a = 1.023	gt = 0.421		0.9981	0.9983	0.01063	0.00927
	50	k = 0.01471	a = 0.9635	gt = 0.2194		0.999		0.00724	
	60	k = 0.02146	a = 0.9762	gt = 0.6785		0.9959		0.01458	
		k = 0.02934	a = 0.9952	gt = 0.01321		0.9991		0.00722	
	70	k = 0.03193	a = 0.9835	gt = 0.5799		0.9994		0.00669	
	80								

Relative analysis was carried out to evaluate the model's validity. Between the actual and anticipated data, there was an outstanding correlation with an R^2 value of 0.9991 (**Fig. 3.2**). There is a residual graphic that corresponds to this in **Fig. 3.3**. When the total fit was taken into account, it was found that the residuals are extremely close to zero and are randomly distributed, which shows the fit is good [28, 80].

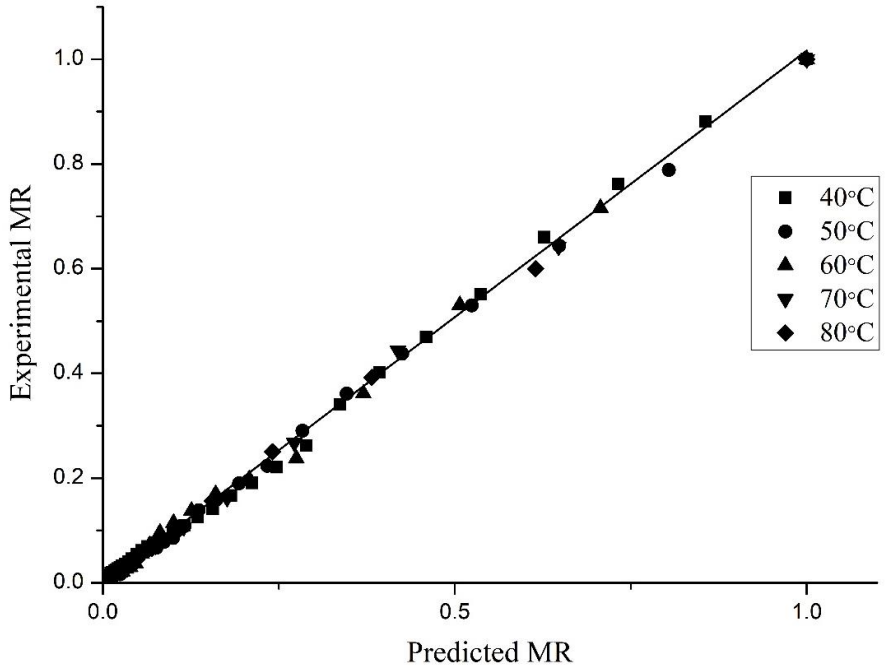

Fig. 3.2. Plot for experimental vs predicted MR for 'Approximation of diffusion' model

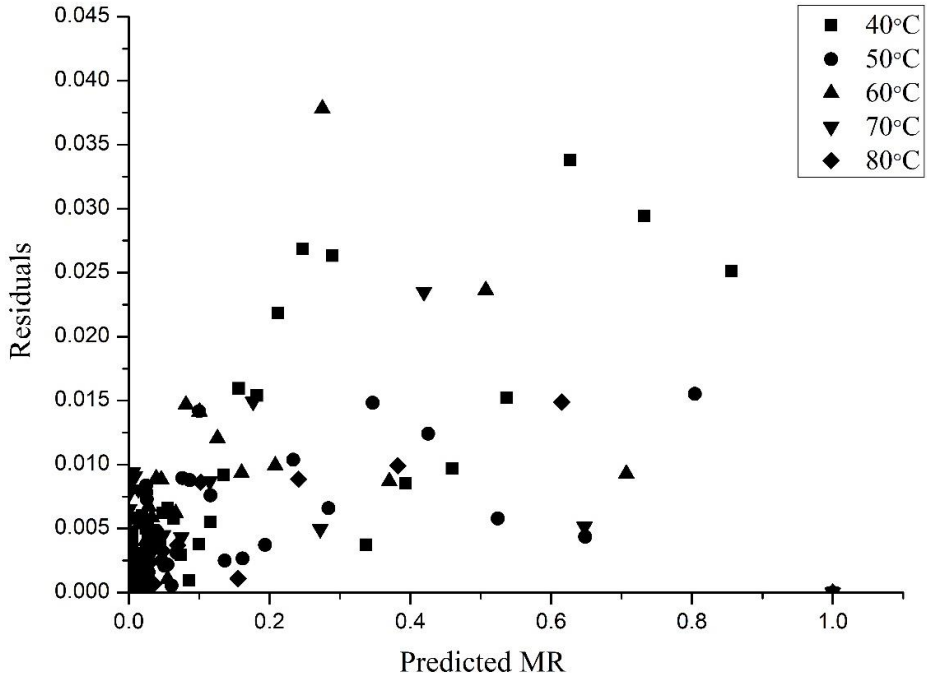

Fig. 3.3. Residual analysis plot

3.3.4. Effective moisture diffusivity

The average effective moisture diffusivity was obtained by calculating the arithmetic mean of the effective moisture diffusivities that were determined for varying moisture contents during the drying process as shown in **Fig. 3.4**.

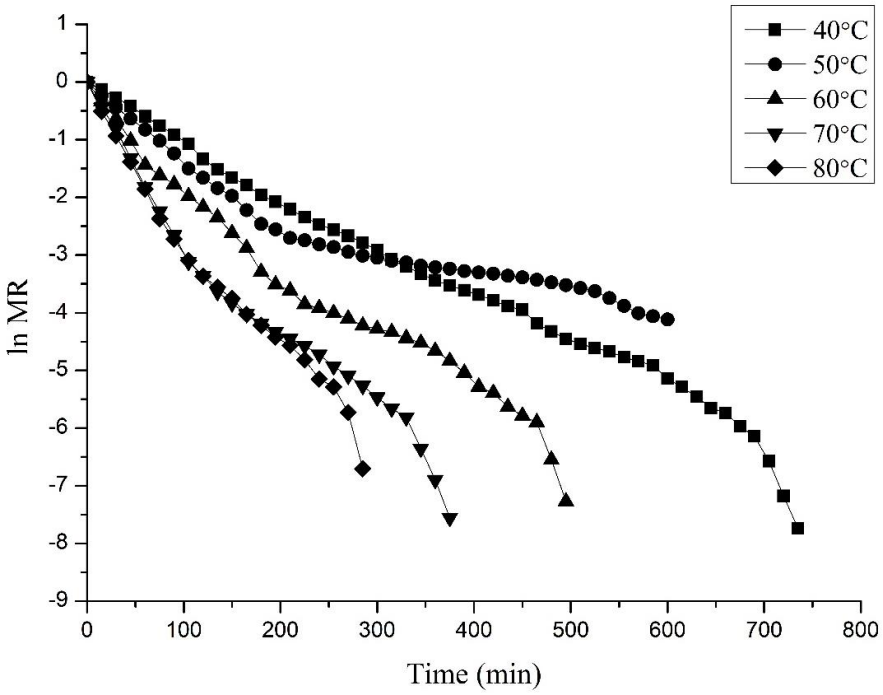

Fig. 3.4. Plot for ln(MR) vs drying time

The effective moisture diffusivity (D_{eff}) was found to range between 1.02596×10^{-11} and 7.7272×10^{-11} m^2/s for the convective drying of *T. chebula* fruit from 40 to 80 °C (**Table 3.5**).

Table 3.5. Diffusivity of *T. chebula* fruit during drying at different temperatures

Temperature (°C)	Diffusivity (m^2/s)	R^2
40	1.02596×10^{-11}	0.9973
50	1.63856×10^{-11}	0.9966
60	3.10503×10^{-11}	0.9985
70	5.27058×10^{-11}	0.9993
80	7.72720×10^{-11}	0.9988

In this objective, effective diffusivities obtained were in the approved range of 10^{-12} to 10^{-8} generally observed for biological materials [25, 84]. With increase in the drying temperature the effective moisture diffusivities were found to increase greatly.

3.3.5. Activation energy

The plot for ln (D_{eff}) vs reciprocal of the temperature (1/T) is presented in **Fig. 3.5** and was used for calculating the activation energy.

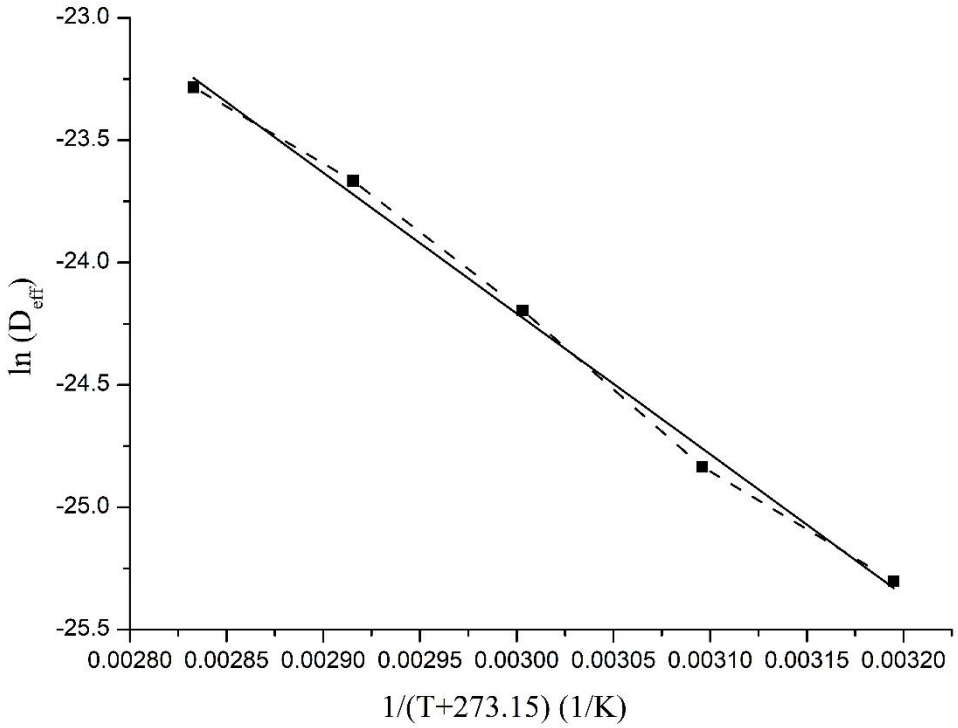

Fig. 3.5. Arrhenius plot for ln(D_{eff}) vs inverse of temperature for drying of fruit

Thus, the value of activation energy in this study is found to be 47.87 kJ/mol which is within the range of 12.7-110 kJ/mol as observed by Zogzas et al. [84] for various food materials. The E_a obtained for *T. chebula* fruit was found to be comparable to figs which is in the range of 30.8-48.47 as reported by Babalis and Belessiotis [9].

3.3.6. Degradation kinetics of TPC, TFC, vitamin C, DPPH during drying

The importance of vitamin C and phenolic compounds in human nutrition and their advantages for health are well known. Indicators of quality are employed with these elements in a number of food processing operations. The stability of these chemicals is temperature-dependent and rapidly lost during drying. Therefore, it is crucial to research how these molecules degrade throughout the drying process. **Fig. 3.6-3.9**, show the decrease in antioxidant activity during drying and the degradation of vitamin C, total phenols, and total flavonoids. Initial concentrations of TPC, TFC, vitamin C, and DPPH radical scavenging activity were 196.26 mg GAE/g of pulp (dry weight), 88.40 mg QE/g of pulp (dry weight), 708.24 mg/100 g pulp (dry weight), and 97.01%, found in the *T. chebula* fruit respectively. TPC, TFC, Vitamin C and DPPH radical scavenging activity decreased with time and their degradation followed a first order kinetics model.

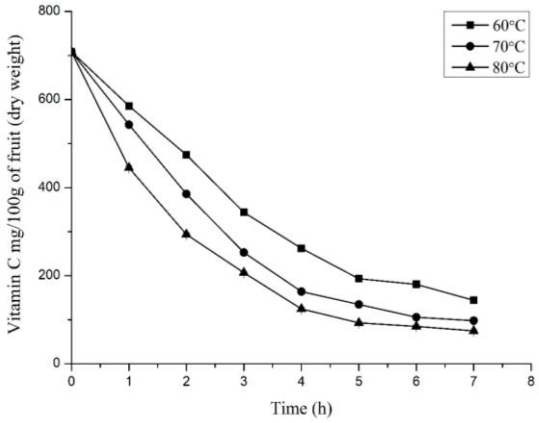

Fig. 3.6. Variation in vitamin C during drying at different temperatures

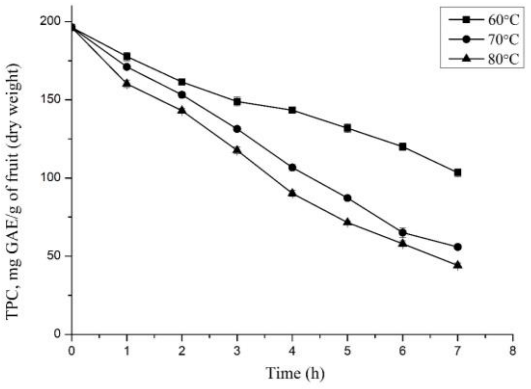

Fig. 3.7. Variation in TPC during drying at different temperatures

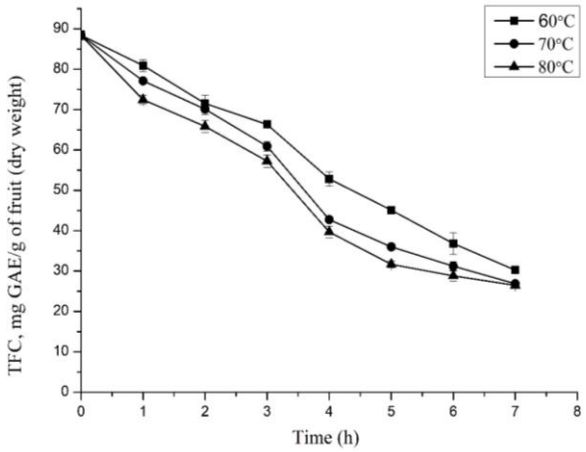

Fig. 3.8. Variation in TFC during drying at different temperatures

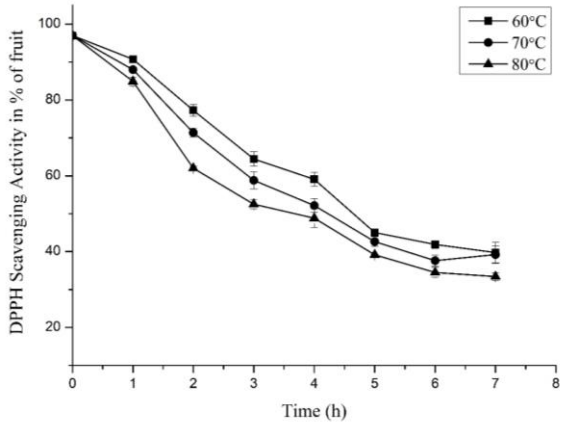

Fig. 3.9. Variation in antioxidant activity during drying at different temperatures

The 'k', 'R^2', '$t_{1/2}$' values at various temperatures and the 'E_a' for the different component are shown in **Table 3.6**. The rate of vitamin C degradation was significantly higher than TPC, TFC, or antioxidant activity, as can be seen from the "k" values for the various components. For all the components, the rate of degradation likewise increased with temperature. Furthermore, it was found that for TPC and TFC, the deterioration rate increased dramatically when the temperature was raised from 60 to 70 °C, but did not alter significantly when the temperature was raised further to 80 °C. For all temperatures, there were sizable variations in the vitamin C and antioxidant activity "k" values. Haritaki pulp mostly results from the presence of vitamin C, with other components contributing

less to antioxidant action than vitamin C. Half-life ($t_{1/2}$) of each individual component were discovered to shorten with rising drying temperatures. At all temperatures, vitamin C had the lowest $t_{1/2}$. At 60 °C, the $t_{1/2}$ of TPC was found to be 8.31 h, suggesting that little phenolic degradation takes place. At 80 °C the $t_{1/2}$ of DPPH radical scavenging activity was significantly in comparison to other components. This may be explained by the fact that antioxidant activity is a product of the fruit's overall composition and not just vitamin C, which degrades more quickly at 80 °C. A bigger "E_a" value indicates that temperature has a greater impact on how quickly the component degrades. Vitamin C and TPC degradation was also discovered to be more temperature dependent throughout the drying process compared to TFC and antioxidant activity [73]. Temperature is one of the most crucial elements in the breakdown of vitamin C, which also depends on other parameters like pH, light, oxygen, the presence of metals, and enzymes [79]. The 'E_a' for vitamin C in the present study was 25.81 kJ/mol in the temperature range of 60–80 °C which was found to be closer to that obtained by Lien [43] for germinated soy flour in the temperature range of 40-70 °C.

3.3.7. Kinetics of change in colour during drying

The total colour difference (ΔE*) was measured after every 1 h during drying at three different temperatures. The variation in ΔE* with time of drying is shown in **Fig. 3.10** ΔE* increased with time of drying for all temperatures.

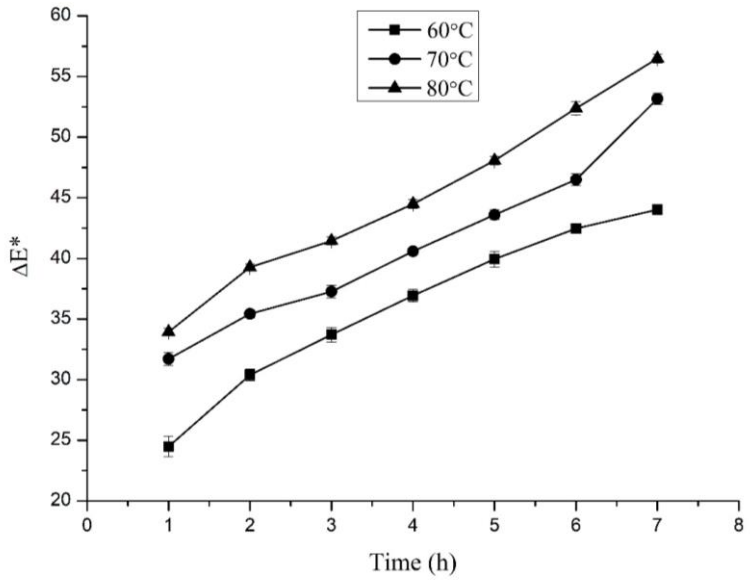

Fig. 3.10. Variation in total colour during drying at different temperatures

With a positive "k" value, the change in E_a followed a first order kinetics, showing that the colour difference from the fresh sample grew as drying time rose (**Table 3.6**). The "k" values for colour change ranged from (0.0794 to 0.0857), and as they are substantially lower than those for vitamin C, TPC, TFC, and DPPH radical scavenging activity, it is clear that drying had little to no impact on the overall colour difference. The colour change "Ea" for *T. chebula* pulp drying was 3.74 kJ/mol, which is extremely low and suggests that colour change is less temperature dependent. The 'k' decreased when temperature was increased from 60 to 80 °C.

Table 3.6. Degradation kinetics parameters and activation energy for phytochemicals and colour of *T. chebula* fruit during drying

Property	Temperature (°C)	k	R^2	$t_{1/2}$ (h)	E_a (kJ/mol)
Vitamin C content	60	-0.2409	0.9921	2.88	25.81
	70	-0.3294	0.9924	2.10	
	80	-0.4081	0.9923	1.70	
TPC	60	-0.0834	0.9874	8.31	42.52
	70	-0.1684	0.9820	4.12	
	80	-0.1980	0.9898	3.50	
TFC	60	-0.1423	0.9746	4.87	12.43
	70	-0.1716	0.9941	4.04	
	80	-0.1833	0.9776	3.78	
DPPH radical scavenging activity	60	-0.1160	0.9856	5.97	13.83
	70	-0.1310	0.9892	5.29	
	80	-0.1540	0.9526	4.50	
Total color difference (ΔE)	60	0.0857	0.9397	8.09	3.74
	70	0.0816	0.9859	8.49	
	80	0.0794	0.9914	8.73	

This demonstrates that pulp colour is better preserved at higher drying temperatures. Fruits and vegetables typically include enzymes like polyphenol oxidase, which causes enzymatic browning. The drop in "k" value with rise in drying temperature may be due to the inactivation of these enzymes at higher temperatures, which reduces enzymatic browning. The '$t_{1/2}$' for colour change was also found to be high and varied from 8.08 to 8.72 h, indicating colour was less affected during the drying process of *T. chebula* fruits.

3.3.8. Moisture Sorption Characteristics of haritaki pulp powder

Because they offer useful guidance for drying, aeration, and storage settings, studies of MSI of foods are significant thermodynamic tools for anticipating the interactions between water and food components [50]. With the aid of the MSI research, information on the maximal stability during packaging and storage can also be forecasted [22]. The sorption isotherms of the powdered haritaki pulp investigated at 30, 40, and 50 °C (EMC against a_w) are shown in **Fig. 3.11**. Moisture sorption isotherms for the haritaki pulp powder followed a j-shaped curve, which is a sign of the type III BET categorization form. The sorption isotherms show that at constant temperature, amorphous materials show an upward in EMC with increased water activity (**Fig. 3.11**). At constant water activity the equilibrium moisture content falls down and rising temperatures, according to experimental results. This behaviour could be caused by a decrease in the total number of water-binding active sites as a result of physical and/or chemical changes brought on by temperature. At increasing temperatures, water molecules become more energetically active, dissociating from the water-binding sites in the meal and reducing the equilibrium moisture content. Since all storage temperatures exhibit an increasing behaviour of adsorption isotherms over the a_w level of 0.65, it is likely that improved storage conditions with a RH of no more than 65% are required for banana flour used in cooking [36]. A rise in the moisture content of the flour may be caused by the fact that culinary banana flour gets starchier when RH approaches 65%. Since moisture cannot diffuse through the crystalline parts of starch (amylopectin), moisture in the flour may affect the structure and act as a plasticizer for the amorphous portion of amylose [7, 36]. In contrast, if aw below 0.3 is maintained for the flour, the mobility of the amorphous amylose area is limited, resulting in a minor plasticization impact [36]. Additionally, it can be inferred that the dielectric effect of water is insufficient to disperse the forces that interact between various sugar molecules at lower a_w levels. On increasing aw, the sugar molecules become more mobile and results in crystallization of amorphous molecules [32].

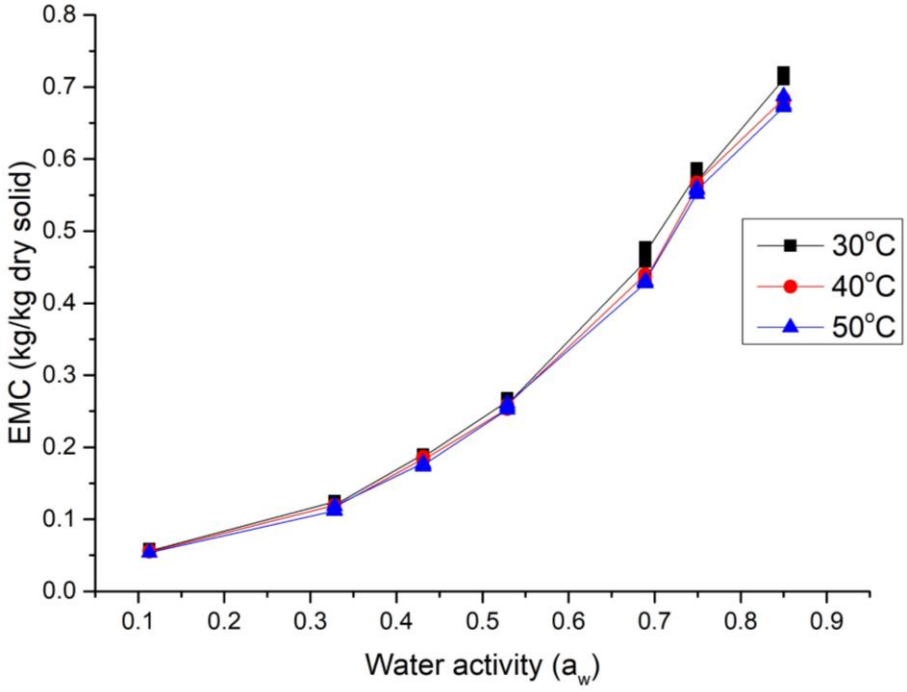

Fig. 3.11. Moisture sorption isotherms of haritaki pulp powder at 30, 40 and 50 °C.

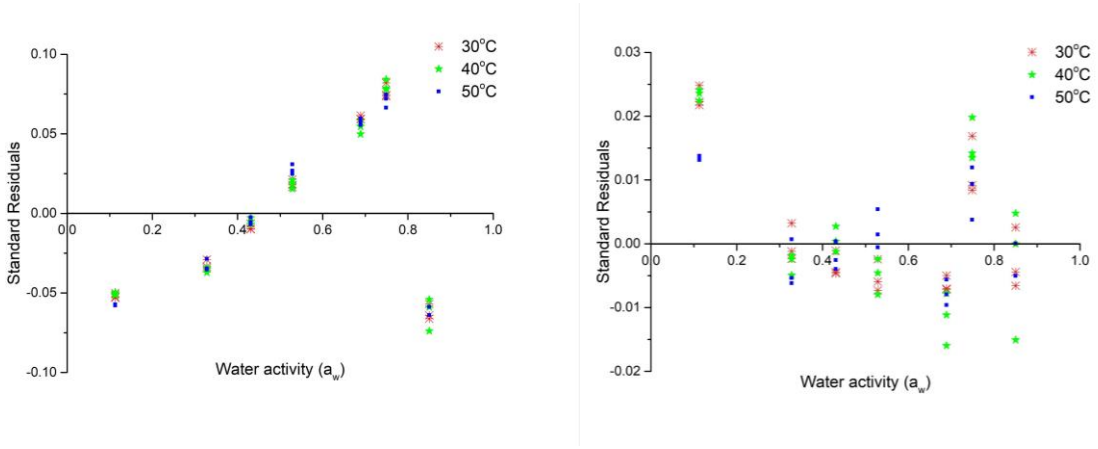

(a) **(b)**

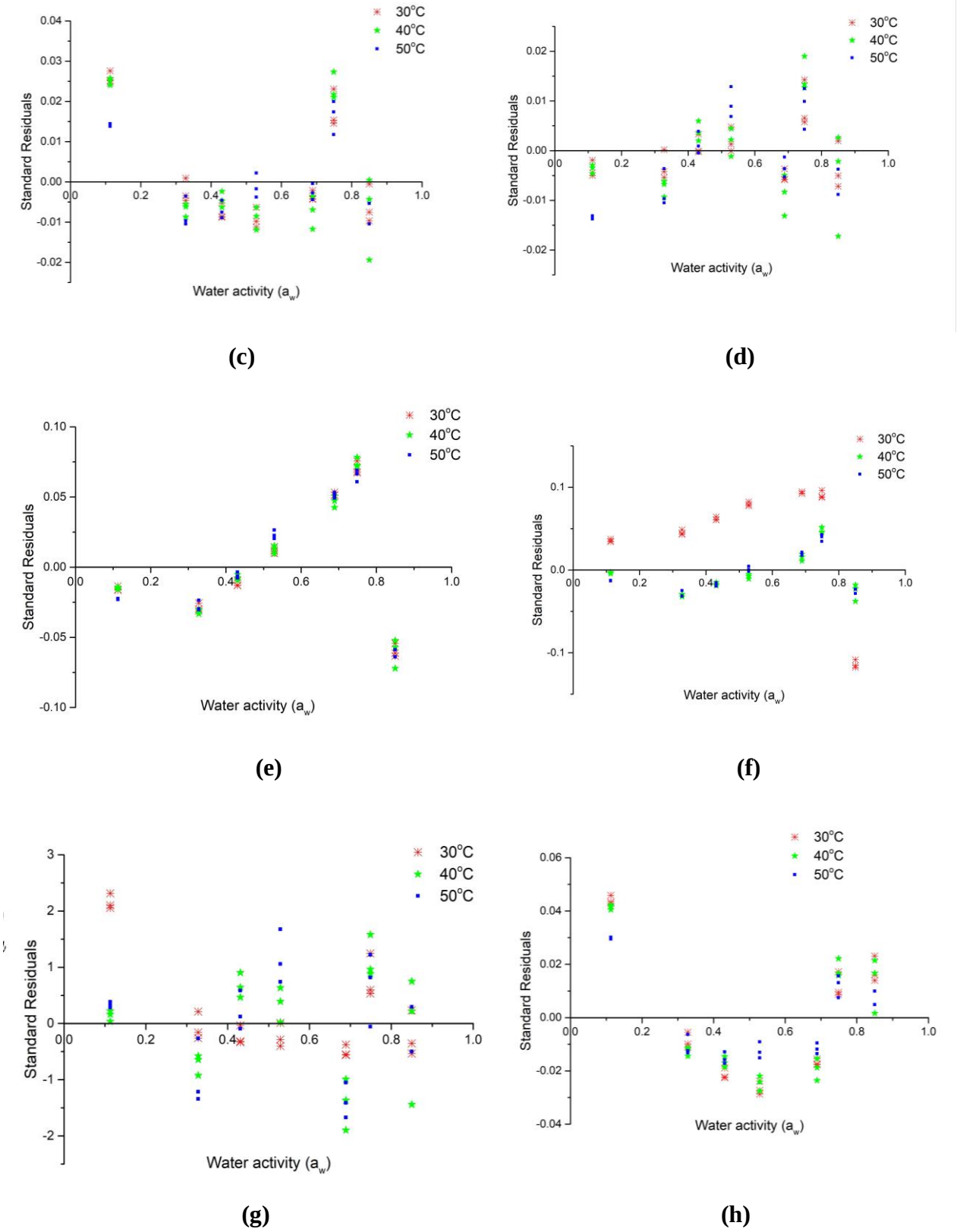

Fig. 3.12. Standardized residuals analysis plot (a) BET Model; (b) GAB model; (c) Modified Henderson Model; (d) Cauri Model; (e) Iglesias and Chirife Model; (f) Modified Oswin Model; (g) Peleg Model; (h) Modified Smith Model

3.3.9. Mathematical Modelling and Fitting of Moisture Sorption Data

Experimental data with an a_w range of 0.11-0.87, conducted at three different temperatures (30-50 °C), was used to fit eight different sorption isotherm models, which are provided in (**Table 3.7** and **Fig. 3.11**). The results of the statistical evaluation of the experimental data of haritaki pulp powder suited to the models of moisture sorption are summarized here. The models with the lowest SSE, χ^2 and highest adjusted R^2 were deemed to be the best fits. Model with adjusted correlation coefficient, R^2_{adj}>0.99 was considered to be best fit. According to the statistical model indices, Peleg model was proved to be best fitted among the eight selected models with highest R^2_{adj} values of greater than 0.997 and smallest χ^2 value of 8.22×10^{-5}. All of the models showed unpredictability in the standardised residual plots, which was regarded as a good fit (**Fig. 3.12**). Comprehensive proof validation of a sorption model requires a mechanistic approach rather than just fitting experimental data to it [18]. The semi-empirical GAB model has fewer biologically important parameters than the fully empirical Peleg model. For the stability of storage, knowledge of the monolayer moisture (M_o) of food goods is essential. Because it denotes a potent water-surface contact, it is an essential metric that guarantees that no related reaction occurs if the moisture content of foods remains below M_o [6]. At 30, 40, and 50 ^oC, the GAB model predicted M_o of 0.35, 0.20, and 0.13%, respectively. The BET model was used to estimate the M_o values under the identical circumstances. The findings showed that the M_o reduced as temperature rose, which was consistent with the increased activation energy. The heat of sorption of the monolayer (GAB parameter C) was greater than that of the multilayer (GAB parameter K). These results show that the Peleg model is the best at satisfying the criteria for having the best fit when compared to all other models. Therefore, it can be concluded that the Peleg model provides a more accurate description of and projection of the EMC of haritaki powder over the examined temperature range. In the MSI investigation, Peleg model revealed that this model was suitable and the best one to use. Peleg model always exhibits equal or even greater appropriateness than GAB model, according to the review of Andrade et al. [8], which validates our findings. As for predicting the EMC of other starchy powders, such as potato [31] and pistachio nut [30] at various storage temperatures, several researchers have discovered the Peleg model to be the most appropriate model. It is wise to draw the conclusion that Peleg is a more palatable and appropriate model to forecast the EMC of haritaki powder in the investigated temperature range.

Table 3.7. Estimated parameters of fitted models to the experimental data for the sorption isotherm of haritaki pulp powder at 30, 40 and 50 ℃

Model	Temperature	Goodness of fit parameters				Model coefficients			
	(℃)	SSE	RMSE	χ^2	R^2_{adj}	A	B	C	D
GAB	30	0.00237	0.01148	1.31×10^{-4}	0.99805	0.35805, M_0	0.72664, C	0.77709, K	-
	40	0.00324	0.01342	1.79×10^{-4}	0.99707	0.2091, M_0	0.62679, C	0.74868, K	-
	50	0.00112	0.0079	6.23×10^{-5}	0.99885	0.1397, M_0	0.62531, C	0.73072, K	-
BET	30	0.03776	0.04458	0.001	0.97059	0.00416, M_0	7.13336, C	-	-
	40	0.03869	0.04513	0.002	0.96688	0.00417, M_0	7.48702, C	-	-
	50	0.03739	0.04436	0.001	0.96356	0.00406, M_0	7.81531, C	-	-
Peleg	30	0.00254	0.01189	1.41×10^{-4}	0.99791	0.87134, k_1	0.51927, k_2	4.85086, n_1	1.2892, n_2
	40	0.0014	0.00907	8.22×10^{-5}	0.99866	1.04018, k_1	0.2017, k_2	3.44841, n_1	0.60512, n_2
	50	$6.99X10^{-4}$	0.00641	4.11×10^{-5}	0.99924	0.88539, k_1	0.26543, k_2	3.59009, n_1	0.83925, n_2
Modified Henderson	30	0.00364	0.01383	1.91×10^{-4}	0.99717	2.24197			
	40	0.0046	0.01555	2.41×10^{-4}	0.99606	2.33726			
	50	0.00203	0.01033	1.06×10^{-4}	0.99802	2.48809			

Cauri	30	$5.71x10^{-4}$	0.00549	3.00×10^{-5}	0.99955	-3.20066	3.52919	-	-
	40	0.00156	0.00908	8.23×10^{-5}	0.99766	-3.21833	3.49525	-	-
	50	0.00149	0.00885	7.84×10^{-5}	0.99755	-3.22561	3.42658	-	-
Iglesias and	30	0.05272	0.05268	0.00277	0.95894	0.0911	0.13869	-	-
Chirife	40	0.05252	0.05258	0.00276	0.95504	0.08934	0.13204	-	-
	50	0.05162	0.05212	0.00272	0.94969	0.08691	0.12342	-	-
Modified	30	0.01259	0.02574	6.62×10^{-4}	0.9902	-9.41728	0.47914	0.99407, N	-
Oswin	40	0.01371	0.0276	7.61×10^{-4}	0.98761	-9.37822	0.48109	0.68666, N	-
	50	0.01172	0.02552	6.51×10^{-4}	0.98794	-9.38355	0.48082	0.6748, N	-
Modified	30	0.01188	0.02501	6.25×10^{-4}	0.99075	-24.52	0.4896	-24.28817	0.49459
Smith	40	0.0112	0.02567	6.58×10^{-4}	0.98929	-24.51809	0.48964	-24.28963	0.49421
	50	0.00534	0.01772	3.13×10^{-4}	0.99419	-24.51605	0.48968	-24.30242	0.49395

3.4. Conclusion

The engineering properties of haritaki were computed with the aid of the current study, and these engineering qualities will be useful for designing fruit-related equipment including hoppers, chutes, sorters, and grading machines. The engineering properties are helpful in providing academics and enterprises with extensive knowledge for haritaki fruit post-harvest activities. Deseeded *T. chebula* fruits were dried until the moisture content remained consistent at a range of temperatures (40-60 °C). Different mathematical models were used to fit the data, and it was discovered that the 'approximation diffusion model' provided the best fit. The activation energy was discovered to be 47.87 kJ/mol and the drying rate constant 'k' increased with rise in temperature, demonstrating substantial temperature sensitivity of the process. Along with antioxidant activity and colour change during drying, the kinetics of vitamin C degradation, total phenol and flavonoid concentration, and antioxidant activity were assessed. Following first order kinetics, phytochemicals degraded and changed colour, and the rate of decomposition accelerated with rising temperature. The higher "E_a" value for vitamin C indicates that it degraded more quickly during drying compared to TPC and TFC and that it was also more temperature dependent. One intriguing finding was that colour change decreased as temperature increased. From the findings, it can be inferred that while the rate of drying increased with temperature, the degradation of the phytochemicals also did so, and that temperature had the greatest impact on vitamin C. Therefore, the ideal drying temperature should be chosen based on the final quality requirements for a minimum drying time. By using several salt solutions with different water activities at three distinct storage temperatures. The BET classification of the isotherms was type III. Over the range of water activity and study temperature, the Peleg model provided the best fit to the experimental data on sorption.

3.5. References

1. Akdaş, S., and Başlar, M. Dehydration and degradation kinetics of bioactive compounds for mandarin slices under vacuum and oven drying conditions. *Journal of Food Processing and Preservation*, 39(6), 1098-1107, 2015.
2. Akpinar, E. K. Energy and exergy analyses of drying of red pepper slices in a convective type dryer. *International Communications in Heat and Mass Transfer*, 31(8), 1165-1176, 2004.
3. Akpinar, E. K. Mathematical modelling of thin layer drying process under open sun of some aromatic plants. *Journal of Food Engineering*, *77*(4), 864-870, 2006.
4. Akpinar, E. K., and Bicer, Y. Mathematical modelling of thin layer drying process of long green pepper in solar dryer and under open sun. *Energy Conversion and Management*, 49(6), 1367-1375, 2008.
5. Al-Muhtaseb, A. H., McMinn, W. A. M., and Magee, T. R. Shrinkage, density and porosity variations during the convective drying of potato starch gel. In *14th International Drying Symposium (IDS), São Paulo, Brazil* (Vol. 100, pp. 1604-1611), 2004.
6. Al-Muhtaseb, A. H., Mc-Minn, W. A. M., and Magee, T. R. A. Moisture sorption isotherm characteristics of food products: a review. *Food and bioproducts processing*, 80(2), 118-128, 2002.
7. Al-Muhtaseb, A. H., McMinn, W. A. M., and Magee, T. R. A. Water sorption isotherms of starch powders: part 1: mathematical description of experimental data. *Journal of food Engineering*, 61(3), 297-307, 2004.
8. Andrade, R. D., Lemus, R., and Perez, C. E. Models of sorption isotherms for food: uses and limitations. *Vitae*, 18(3), 325-334, 2011.
9. Babalis, S. J., and Belessiotis, V. G. Influence of the drying conditions on the drying constants and moisture diffusivity during the thin-layer drying of figs. *Journal of food Engineering*, 65(3), 449-458, 2004.
10. Bal, S., and Mishra, H. N. Engineering properties of soybean. In *Proceedings of the national seminar on soybean processing and utilization in India* (pp. 146-165), 1988.
11. Belghit, A., Kouhila, M., and Boutaleb, B. C. Experimental study of drying kinetics by forced convection of aromatic plants. *Energy Conversion and Management*, 41(12), 1303-1321, 2000.

12. Brand-Williams, W., Cuvelier, M. E., and Berset, C. L. W. T. Use of a free radical method to evaluate antioxidant activity. *LWT-Food science and Technology*, 28(1), 25-30, 1995.
13. Brennan, J. G., and Grandison, A. S. (Eds.). Food processing handbook, 2012.
14. Brunauer, S., Emmett, P. H., and Teller, E. Adsorption of gases in multimolecular layers. *Journal of the American chemical society*, 60(2), 309-319, 1938.
15. Burubai, W., and Amber, B. Some physical properties and proximate composition of Ipoli fruits. *Journal of Food Processing and Technology*, 5(7), 2014.
16. Caurie, M. Derivation of full range moisture sorption isotherms. Water activity: influences on food quality: a treatise on the influence of bound and free water on the quality and stability of foods and other natural products, 63-87, 1981.
17. Chirife, J., and Iglesias, H. A. Equations for fitting water sorption isotherms of foods: Part 1—a review. *International Journal of Food Science & Technology*, 13(3), 159-174, 1978.
18. Chirife, J., Timmermann, E. O., Iglesias, H. A., and Boquet, R. Some features of the parameter k of the GAB equation as applied to sorption isotherms of selected food materials. *Journal of Food Engineering*, 15(1), 75-82, 1992.
19. Chong, C. H., Law, C. L., Cloke, M., Hii, C. L., Abdullah, L. C., and Daud, W. R. W. Drying kinetics and product quality of dried Chempedak. *Journal of Food Engineering*, 88(4), 522-527, 2008.
20. Debnath, S., Hemavathy, J., and Bhat, K. K. Moisture sorption studies on onion powder. *Food Chemistry*, 78(4), 479-482, 2002.
21. Dewanto, V., Wu, X., Adom, K. K., and Liu, R. H. Thermal processing enhances the nutritional value of tomatoes by increasing total antioxidant activity. *Journal of agricultural and food chemistry*, 50(10), 3010-3014, 2002.
22. Doporto, M. C., Dini, C., Mugridge, A., Viña, S. Z., and García, M. A. Physicochemical, thermal and sorption properties of nutritionally differentiated flours and starches. *Journal of Food Engineering*, 113(4), 569-576, 2012.
23. Dorneles, L. D. N. S., Goneli, A. L. D., Cardoso, C. A. L., da Silva, C. B., Hauth, M. R., Oba, G. C., and Schoeninger, V. Effect of air temperature and velocity on drying kinetics and essential oil composition of Piper umbellatum L. leaves. *Industrial Crops and Products*, 142, 111846, 2019.
24. Doymaz, I. Thin-layer drying behaviour of mint leaves. *Journal of Food Engineering*, 74(3), 370-375, 2006.

25. Doymaz, İ. Drying kinetics, rehydration and colour characteristics of convective hot-air drying of carrot slices. *Heat and Mass Transfer*, 53(1), 25-35, 2017.
26. Fang, S., Wang, Z., and Hu, X. Hot air drying of whole fruit Chinese jujube (*Zizyphus jujuba Miller*): thin-layer mathematical modelling. *International journal of food science & technology*, 44(9), 1818-1824, 2009.
27. Fontan, C. F., Chirife, J., Sancho, E., and Iglesias, H. A. Analysis of a model for water sorption phenomena in foods. *Journal of Food Science*, 47(5), 1590-1594, 1982.
28. Ghaderi, A., Abbasi, S., Motevali, A., and Minaei, S. Comparison of mathematical models and artificial neural networks for prediction of drying kinetics of mushroom in microwave-vacuum drier. *Chemical Industry and Chemical Engineering Quarterly/CICEQ*, 18(2), 283-293, 2012.
29. Goyal, R. K., Kingsly, A. R. P., Manikantan, M. R., and Ilyas, S. M. Mathematical modelling of thin layer drying kinetics of plum in a tunnel dryer. *Journal of food Engineering*, 79(1), 176-180, 2007.
30. Hayoglu, I., and Faruk Gamli, O. Water sorption isotherms of pistachio nut paste. *International journal of food science & technology*, 42(2), 224-227, 2007.
31. Iguedjtal, T., Louka, N., and Allaf, K. Sorption isotherms of potato slices dried and texturized by controlled sudden decompression. *Journal of Food Engineering*, 85(2), 180-190, 2008.
32. Johnson, P. T., and Brennan, J. G. Moisture sorption isotherm characteristics of plantain (Musa, AAB). *Journal of Food Engineering*, *44*(2), 79-84, 2000.
33. Juang, L. J., Sheu, S. J., and Lin, T. C. Determination of hydrolyzable tannins in the fruit of *Terminalia chebula* Retz. by high-performance liquid chromatography and capillary electrophoresis. *Journal of Separation Science*, 27(9), 718-724, 2004.
34. Kaya, S., and Kahyaoglu, T. Moisture sorption and thermodynamic properties of safflower petals and tarragon. *Journal of Food Engineering*, 78(2), 413-421, 2007.
35. Keneni, Y. G., Hvoslef-Eide, A. T., and Marchetti, J. M. Mathematical modelling of the drying kinetics of Jatropha curcas L. seeds. *Industrial crops and products*, 132, 12-20, 2019.
36. Khawas, P., and Deka, S. C. Moisture sorption isotherm of underutilized culinary banana flour and its antioxidant stability during storage. *Journal of Food Processing and Preservation*, 41(4), 2017.

37. Khwaja, O., Siddiqui, M. H., and Younis, K. Underutilized kadam (*Neolamarckia cadamba*) fruit: Determination of some engineering properties and drying kinetics. *Journal of the Saudi Society of Agricultural Sciences*, 19(6), 401-408, 2020.
38. Kim, D. O., Jeong, S. W., and Lee, C. Y. Antioxidant capacity of phenolic phytochemicals from various cultivars of plums. *Food chemistry*, 81(3), 321-326, 2003.
39. Koç, B., Yilmazer, M. S., Balkır, P., and Ertekin, F. K. Moisture sorption isotherms and storage stability of spray-dried yogurt powder. *Drying Technology*, 28(6), 816-822, 2010.
40. Kooli, S., Fadhel, A., Farhat, A., and Belghith, A. Drying of red pepper in open sun and greenhouse conditions: mathematical modeling and experimental validation. *Journal of food engineering*, 79(3), 1094-1103, 2007.
41. Kubola, J., Siriamornpun, S., and Meeso, N. Phytochemicals, vitamin C and sugar content of Thai wild fruits. *Food Chemistry*, 126(3), 972-981, 2011.
42. Labuza, T. P. Application of chemical kinetics to deterioration of foods, 1984.
43. Lien, D. T. P. Drying kinetics and thermal degradation of phenolic compounds and vitamin C in full fat germinated soy flours. *International Journal of Food Sciences and Nutrition*, 2(1), 10-14, 2017.
44. Martínez-Las Heras, R., Heredia, A., Castelló, M. L., and Andrés, A. Moisture sorption isotherms and isosteric heat of sorption of dry persimmon leaves. *Food Bioscience*, 7, 88-94, 2014.
45. Meziane, S. Drying kinetics of olive pomace in a fluidized bed dryer. *Energy Conversion and Management*, 52(3), 1644-1649, 2011.
46. Midilli, A. D. N. A. N., Kucuk, H. A. Y. D. A. R., and Yapar, Z. İ. Y. A. A new model for single-layer drying. *Drying technology*, 20(7), 1503-1513, 2002.
47. Minguez-Mosquera, M. I., Jaren-Galan, M., and Garrido-Fernandez, J. Influence of the industrial drying processes of pepper fruits (*Capsicum annuum Cv. Bola*) for paprika on the carotenoid content. *Journal of Agricultural and Food Chemistry*, 42(5), 1190-1193, 1994.
48. Modi, S. K., Durgaprasad, B., and Basavaraj, M. An experimental study on drying kinetics of guava fruit (*Psidium Guajava* L.) by thin layer drying. *J. Environ. Sci. Toxicol. Food Technol*, 9(1), 74-80, 2015.
49. Mujumdar, A. S., and Law, C. L. Drying technology: Trends and applications in postharvest processing. *Food and Bioprocess Technology*, 3(6), 843-852, 2010.

50. Mundada, M., and Hathan, B. S. Studies on moisture sorption isotherms for osmotically pretreated and air-dried pomegranate arils. *Journal of Food Processing and Preservation*, 36(4), 329-338, 2012.
51. Mwithiga, G., and Jindal, V. K. Physical changes during coffee roasting in rotary conduction-type heating units. *Journal of Food Process Engineering*, 26(6), 543-558, 2003.
52. Naik, G. H., Priyadarsini, K. I., Naik, D. B., Gangabhagirathi, R., and Mohan, H. Studies on the aqueous extract of *Terminalia chebula* as a potent antioxidant and a probable radioprotector. *Phytomedicine*, 11(6), 530-538, 2004.
53. Ong, S. P., and Law, C. L. Drying kinetics and antioxidant phytochemicals retention of salak fruit under different drying and pretreatment conditions. *Drying Technology*, 29(4), 429-441, 2011.
54. Page, G. E. *Factors Influencing the Maximum Rates of Air Drying Shelled Corn in Thin layers*. Purdue University, 1949.
55. Panchariya, P. C., Popovic, D., and Sharma, A. L. Thin-layer modelling of black tea drying process. *Journal of food engineering*, 52(4), 349-357, 2002.
56. Patel, M., Pradhan, R., and Naik, S. Physical properties of fresh mahua. *International Agrophysics*, 25(3), 2011.
57. Peleg, M. Assessment of a semi-empirical four parameter general model for sigmoid moisture sorption isotherms. *Journal of Food Process Engineering*, 16(1), 21-37, 1993.
58. Peng, G., Chen, X., Wu, W., and Jiang, X. Modeling of water sorption isotherm for corn starch. *Journal of Food Engineering*, 80(2), 562-567, 2007.
59. Pradhan, R. C., Said, P. P., and Singh, S. (2013). Physical properties of bottle gourd seeds. *Agricultural Engineering International: CIGR Journal*, 15(1), 106-113, 2013.
60. Ranganna, S. *Handbook of analysis and quality control for fruit and vegetable products*. Tata McGraw-Hill Education, 1986.
61. Rathinamoorthy, R., and Thilagavathi, G. Optimisation of process conditions of cotton fabric treatment with *Terminalia chebula* extract for antibacterial application, 2013.
62. Rifna, E. J., and Dwivedi, M. Optimization and validation of microwave–vacuum drying process variables for recovery of quality attribute and phytochemical properties in pomegranate peels (*Punica granatum L. cv. Kabul*). *Journal of Food Measurement and Characterization*, 15(5), 4446-4464, 2021.

63. Sahay, K. M., and Singh, K. K. *Unit operations of agricultural processing*. Vikas Publishing House Pvt. Ltd. 1996.
64. Saleem, A., Husheem, M., Härkönen, P., and Pihlaja, K. Inhibition of cancer cell growth by crude extract and the phenolics of *Terminalia chebula* retz. fruit. *Journal of Ethnopharmacology*, 81(3), 327-336, 2002.
65. Shahbazi, F., and Rahmati, S. Mass modeling of fig (*Ficus carica* L.) fruit with some physical characteristics. *Food Science & Nutrition*, 1(2), 125-129, 2013.
66. Singh, A., Bajpai, V., Kumar, S., Kumar, B., Srivastava, M., and Rameshkumar, K. B. Comparative profiling of phenolic compounds from different plant parts of six *Terminalia* species by liquid chromatography–tandem mass spectrometry with chemometric analysis. *Industrial Crops and Products*, 87, 236-246, 2016.
67. Sivabalan, K., Sunil, C. K., and Venkatachalapathy, N. Mass modeling of coconut (*Cocos nucifera* L.) with physical characteristics. *IJCS*, 7(3), 5067-5072, 2019.
68. Sormoli, M. E., and Langrish, T. A. Moisture sorption isotherms and net isosteric heat of sorption for spray-dried pure orange juice powder. *LWT-Food Science and Technology*, 62(1), 875-882, 2015.
69. Thompson, R. F. Foundations of physiological psychology, 1967.
70. Tulek, Y. Drying kinetics of oyster mushroom (*Pleurotus ostreatus*) in a convective hot air dryer. *Journal of Agricultural Science and Technology*, 13(5), 655-664, 2011.
71. Van den Berg, C. *Vapour sorption equilibria and other water-starch interactions: A physico-chemical approach*. Wageningen University and Research, 1981.
72. Van den Berg, C., and Bruin, S. In Water Activity: Influences on Food quality (LB Rockland, GF Stewart, eds), 1-61, 1981.
73. Vardin, H., and Yilmaz, F. M. The effect of blanching pre-treatment on the drying kinetics, thermal degradation of phenolic compounds and hydroxymethyl furfural formation in pomegranate arils. *Italian journal of food science*, 30(1), 2018.
74. Varghese K, S. H. I. B. Y., Ramachandrannair, S. V., and Mishra, H. N. Moisture sorption characteristics of curd (Indian yogurt) powder. *International journal of dairy technology*, 62(1), 85-92, 2009.
75. Vega-Gálvez, A., Zura-Bravo, L., Lemus-Mondaca, R., Martinez-Monzó, J., Quispe-Fuentes, I., Puente, L., and Di Scala, K. Influence of drying temperature on dietary fibre, rehydration properties, texture and microstructure of Cape gooseberry (*Physalis peruviana* L.). *Journal of Food Science and Technology*, 52(4), 2304-2311, 2015.

76. Verma, L. R., Bucklin, R. A., Endan, J. B., and Wratten, F. T. Effects of drying air parameters on rice drying models. *Transactions of the ASAE*, 28(1), 296-0301, 1985.
77. Viswanathan, R., Jayas, D. S., and Hulasare, R. B. Sorption isotherms of tomato slices and onion shreds. *Biosystems Engineering*, 86(4), 465-472, 2003.
78. Westerman, P. W., White, G. M., and Ross, I. J. Relative humidity effect on the high-temperature drying of shelled corn. *Transactions of the ASAE*, *16*(6), 1136-1139, 1973.
79. Williams, J. T. *Global research on underutilized crops: An assessment of current activities and proposals for enhanced cooperation*. Bioversity International, 2002.
80. Wisniak, J., and Polishuk, A. Analysis of residuals—a useful tool for phase equilibrium data analysis. *Fluid Phase Equilibria*, 164(1), 61-82, 1999.
81. Wu, B., Ma, H., Qu, W., Wang, B., Zhang, X., Wang, P., and Pan, Z. Catalytic infrared and hot air dehydration of carrot slices. *Journal of food process engineering*, 37(2), 111-121, 2014.
82. Xiao, H. W., Pang, C. L., Wang, L. H., Bai, J. W., Yang, W. X., and Gao, Z. J. Drying kinetics and quality of Monukka seedless grapes dried in an air-impingement jet dryer. *Biosystems Engineering*, 105(2), 233-240, 2010.
83. Yaldiz, O., Ertekin, C., and Uzun, H. I. Mathematical modeling of thin layer solar drying of sultana grapes. *Energy*, 26(5), 457-465, 2001.
84. Zogzas, N. P., Maroulis, Z. B., and Marinos-Kouris, D. Moisture diffusivity data compilation in foodstuffs. *Drying technology*, 14(10), 2225-2253, 1996.